The VIIRS-CrIS Data Fusion project: Construction of Infrared Absorption Spectral Bands for VIIRS

Data product user guide and file specification document

This guide is specific to Version 2.0 of the VIIRS-CrIS Data Fusion product

Version 2.0

December 2021

Contents

1 Introduction

This document is designed to provide relevant information to users of the Suomi-National Polar-Orbiting Partnership (S-NPP) Visible Infrared Imaging Radiometer Suite (VIIRS) infrared (IR) absorption bands. It contains some background information about the data fusion approach using a combination of VIIRS and CrIS (Crosstrack Infrared Sounder) and lists and explains the content of the data files.

The primary data products are orbit-level (Level-2, L2) of VIIRS IR absorption band radiances and brightness temperatures. Other geophysical quantities and related ancillary information are also provided. More specifically, we construct narrowband radiances using an imager-sounder data fusion process (see references) that adopts the Aqua MODIS spectral response functions for MODIS bands 23–25 (in the 4.5-μm CO_2 band), 27 & 28 (in the H_2O band), 30 (in the O_3 band), 31 & 32 (11 and 12-μm window bands) and 33–36 (in the 15-μm CO_2 band).

The L2 files also include radiances for the bowtie-deleted pixels that are present in the original VIIRS L1B files. The bowtie-deleted pixels are filled using a nearest-neighbor technique. We fill these pixels in anticipation of their use in various cloud retrieval methods that use a pixel array to calculate, for example, a mean and standard deviation to help assess homogeneity. All data files are in Network Common Data Format Version-4 (NetCDF4) and include metadata compliant with the Climate and Forecast (CF) conventions version 1.6. Note that these NetCDF4 files are also accessible via HDF5 libraries.

1.1 Algorithm background

Details of the methodology and simultaneous nadir overpass pixel comparisons between VIIRS and Aqua MODIS are provided in papers or presentations. Please contact us if you have questions about performance and likely issues within your specific application of interest.

Additional information, including links to relevant papers, is available in the References section at the end of this document and at the VIIRS-CrIS Data Fusion project website (http://stc-se.com/data/bbaum/Baum-DataFusion).

1.2 What is new in Version 2.0

In working with the VIIRS+CrIS radiance fusion product, a number of relatively minor improvements have been made to increase the granule yield and also take advantage of the latest updates to the VIIRS and CrIS calibration. These improvements have come through collaboration with members of the CERES Science Team and the VIIRS and CrIS calibration teams. We note that the calibration for both VIIRS and CrIS has been improved since the v1.0 Fusion radiance product (for S-NPP and NOAA-20) started production in 2019 Fall.

The fusion granule yield for Version 1.0.1 is shown in Figure 1 for Suomi-NPP for two years: 2017 and 2018. Figure 2 shows the Version 1.0.1 yield for NOAA-20 for years 2018 and 2019. The VIIRS data were not fully available at the beginning of the record for NOAA-20 (February

2018) but this was only temporary. This document will be updated to include the granule yield for Version 2.0 when it is available.

Note that for Suomi-NPP, there are noticeable gaps in the yield that occur quarterly. Such gaps are primarily due to the VIIRS Black Body Warm-Up and Cool-Down (BB WUCD) operations. The WUCD operations have been occurring quarterly for Suomi-NPP since it launched in 2012 through mid-2018 but since then, these operations have only been run once per year. These WUCD calibration operations have not been performed for NOAA-20 since March, 2018. In discussions with the VIIRS calibration team, the Suomi-NPP 11-μm brightness temperatures are only very slightly impacted in a WUCD procedure (about 0.1K). We now construct the VIIRS+CrIS fusion radiance product during these procedures as much as possible. The yield is improved for Suomi-NPP but there are still missing granules during these WUCD periods. Fortunately, NOAA-20 does not have these data gaps.

2018 98% available

Day	1	2	3	4	5	6	7	8	9	10	11	12	13	14	15	16	17	18	19	20	21	22	23	24	25	26	27	28	29	30	31	Total
Dec	100	100	100	100	100	100	100	100	100	100	100	100	100	100	100	100	100	98	100	100	100	100	100	100	100	100	100	100	100	100	100	99
Nov	98	100	100	100	100	100	100	100	100	100	100	100	100	100	100	100	100	99	98	100	100	100	100	100	100	100	100	100	100	100		99
Oct	100	100	100	100	100	100	100	100	100	100	100	100	100	100	100	100	100	100	100	100	100	100	100	100	100	100	100	100	100	100	100	100
Sep	100	100	100	100	100	100	100	100	100	100	100	93	100	100	100	100	100	100	100	100	100	100	100	100	100	100	100	100	100	100		99
Aug	98	100	100	100	100	100	100	100	100	100	100	100	100	100	100	100	100	100	100	100	100	100	100	100	100	100	100	100	100	100	97	99
Jul	100	100	100	100	98	100	100	100	100	100	100	100	100	100	100	97	100	100	100	100	100	100	100	100	100	100	100	100	100	100	100	99
Jun	100	100	100	100	100	100	100	100	100	100	100	100	100	100	100	100	100	24	0	85	100	100	98	100	100	100	100	100	100	100		93
May	100	100	100	100	100	100	100	100	100	100	100	100	100	100	100	100	100	100	100	100	100	100	100	100	98	100	100	100	100	100	100	99
Apr	100	100	100	100	100	100	100	100	100	100	100	100	100	100	100	100	100	100	100	100	100	100	100	100	98	100	100	100	100	100		99
Mar	100	100	100	100	100	100	100	100	100	100	100	24	0	85	100	100	100	100	100	100	100	100	100	100	100	100	98	100	100	100	100	93
Feb	100	100	100	100	100	100	100	100	100	100	100	100	89	100	100	100	100	100	100	100	100	100	100	100	100	98	100	100				99
Jan	91	100	100	100	100	100	100	100	100	100	91	100	100	100	100	100	100	100	100	100	100	100	100	100	100	100	98	100	89	100	100	99

2017 97% available

Day	1	2	3	4	5	6	7	8	9	10	11	12	13	14	15	16	17	18	19	20	21	22	23	24	25	26	27	28	29	30	31	Total
Dec	100	100	100	100	100	100	100	100	100	100	100	100	100	100	100	98	100	24	0	85	100	90	100	100	100	100	100	100	98	94	86	92
Nov	100	100	100	100	100	100	100	100	100	100	100	100	100	100	100	100	100	100	100	100	100	100	100	98	100	100	99	100	97	92		99
Oct	100	100	100	99	100	100	100	100	100	100	100	100	100	100	100	100	100	100	100	100	100	100	100	100	100	100	100	100	100	100	98	99
Sep	100	100	100	59	100	100	100	100	100	100	100	100	100	100	100	100	100	24	0	85	100	100	100	100	100	100	100	99	54	100		90
Aug	100	100	100	100	100	100	100	100	100	100	100	100	100	100	100	100	100	100	100	100	100	100	100	100	100	100	89	100	100	100	100	99
Jul	100	100	100	100	100	100	100	100	100	100	100	99	100	100	100	100	100	100	100	100	100	100	100	100	100	100	100	100	100	100	100	99
Jun	99	100	100	98	100	100	100	100	100	100	100	100	100	100	100	100	100	100	24	0	85	100	100	100	100	100	100	100	100	100		93
May	100	100	100	100	100	97	100	100	100	100	100	100	100	100	100	100	100	100	100	100	100	100	100	100	100	100	100	100	100	100	100	99
Apr	100	100	100	100	98	98	100	100	100	100	100	100	100	100	100	100	100	100	100	100	100	100	100	100	100	100	100	100	100	100		99
Mar	100	100	100	100	100	100	100	98	100	100	100	100	24	0	83	100	100	100	100	100	100	100	100	100	98	89	100	100	100	100	100	93
Feb	100	100	100	100	100	100	98	100	100	100	100	100	100	100	100	100	100	100	100	100	100	100	100	100	100	100	100	100				99
Jan	100	100	100	100	100	100	100	97	100	100	100	100	100	100	100	100	100	100	100	100	100	100	100	100	100	100	100	100	100	100	100	99

Figure 1: Suomi-NPP fusion radiance granule daily yield in percent for years 2017 and 2018 for Version 1.0.1. WUCD (warm-up cool-down) operations were performed quarterly from 2012-2017 and twice in 2018, after which these operations were performed once annually.

2019 99% available

Day	1	2	3	4	5	6	7	8	9	10	11	12	13	14	15	16	17	18	19	20	21	22	23	24	25	26	27	28	29	30	31	Total
Dec	100	100	98	100	100	100	98	100	100	100	100	100	100	100	100	100	100	100	100	100	100	100	100	100	100	100	100	100	100	100	100	99
Nov	100	100	100	100	100	100	98	100	100	100	100	100	100	100	100	100	100	100	98	100	100	100	100	100	100	100	100	100	100	100		99
Oct	100	100	100	100	100	100	100	100	100	100	100	100	100	100	100	100	100	100	100	100	100	100	100	100	100	100	100	100	100	100	100	100
Sep	100	100	100	100	100	100	100	100	100	100	100	100	100	100	100	100	100	100	100	100	100	100	100	100	100	100	100	100	100	100		100
Aug	100	100	100	100	100	100	100	100	100	100	100	100	100	100	100	100	100	100	100	100	100	100	100	100	100	100	100	100	100	100	100	100
Jul	100	100	100	100	100	100	100	100	100	100	100	100	100	100	100	100	100	100	100	100	100	100	100	100	100	100	100	100	100	100	100	100
Jun	100	100	100	100	100	100	100	100	100	100	99	100	98	100	100	100	100	100	100	100	100	100	99	100	100	100	100	100	100	100		99
May	100	100	100	100	100	100	100	100	100	100	100	100	100	98	100	100	100	100	100	100	100	100	100	100	100	100	100	100	100	100	100	99
Apr	100	100	100	100	100	100	100	100	100	95	98	100	100	100	98	100	100	100	100	100	100	100	100	100	100	100	100	100	100	100		99
Mar	100	100	100	100	100	97	100	100	100	100	100	100	100	100	100	100	98	100	100	100	100	100	100	100	100	100	100	100	100	100	100	99
Feb	100	100	100	98	100	100	100	100	100	100	100	100	100	100	98	100	100	100	100	100	100	100	100	100	100	100	100	100				99
Jan	100	100	100	100	100	100	100	100	100	100	100	100	100	100	100	100	97	100	100	100	100	100	100	100	100	100	100	100	100	100	100	99

2018 98% available

Day	1	2	3	4	5	6	7	8	9	10	11	12	13	14	15	16	17	18	19	20	21	22	23	24	25	26	27	28	29	30	31	Total
Dec	100	100	79	100	100	100	98	100	100	100	100	100	98	100	100	100	100	98	100	100	100	100	100	100	100	100	100	100	100	100	100	99
Nov	100	100	100	100	100	100	100	100	100	99	100	100	100	100	100	100	100	100	98	100	100	100	100	100	100	100	100	100	100	100		99
Oct	100	100	100	100	100	100	100	100	100	100	100	100	100	100	100	100	100	100	100	100	100	100	100	100	100	100	100	100	100	100	100	100
Sep	100	100	100	100	100	100	100	100	100	100	100	100	100	100	100	100	100	100	100	100	100	100	100	100	100	100	100	100	100	100		100
Aug	100	100	100	100	100	100	100	100	100	100	98	100	100	100	100	100	100	100	100	100	100	100	100	98	100	100	100	100	100	100	100	99
Jul	100	100	100	100	100	100	100	100	100	100	100	100	98	100	100	100	100	100	42	100	100	100	100	100	100	100	100	100	100	100	100	98
Jun	100	100	100	100	100	100	100	100	100	100	100	100	100	100	100	100	100	100	99	100	100	100	98	100	100	100	100	100	100	100		99
May	100	100	100	100	100	100	100	100	100	100	100	100	100	100	100	100	100	100	100	100	100	100	100	100	98	100	100	100	100	100	100	99
Apr	100	99	100	100	100	100	100	100	100	100	100	100	100	100	100	100	100	100	100	100	100	100	100	100	98	100	98	100	100	100		99
Mar	100	100	97	100	100	100	100	98	100	100	100	59	0	82	100	100	98	100	100	100	100	100	100	100	100	100	98	100	100	100	100	94
Feb	0	0	0	0	0	0	0	0	0	0	0	0	0	0	0	0	99	93	94	96	84	0	0	17	100	98	100	100				88

Figure 2: NOAA-20 fusion radiance granule daily yield in percent for years 2017 and 2018 for Version 1.0.1. NOAA-20 began operations in February 2018 and there was one WUCD (warm-up cool-down) operation performed in March, 2018.

In Version 1.0.1, the VIIRS granule quality check was performed for the entire granule. If more than 50% of the VIIRS pixels were not of sufficient quality, then the data fusion process was not run. The thought was to exclude granules where there are numerous missing scanlines, or noisy data that were of insufficient quality to perform the fusion process, because the VIIRS-CrIS geolocation process (see ATBD or Section 2.3 of this document) becomes suspect. In Version 2.0, this process was modified so that scanlines are checked for quality, rather than the entire granule. We learned that in the lunar calibration process (8-10 times per year), there are granules that are only partially affected, i.e., there may be a block of missing VIIRS scanlines, followed by a block of continuous scanlines for which good calibration are available. We now process those granules that have continuous blocks of good data. When this occurs, the pixels in the scanlines that are missing data are filled with NaNs.

Version 2 also incorporates two improvements to VIIRS-CrIS collocation software. The first improvement addresses failures that occur when VIIRS experiences a scan sync loss event. These events typically cause a sequence of scans with missing geolocation data, which are now simply ignored instead of causing entire granule failures. The other improvement deals with cases where the older collocation code would miss VIIRS pixels that should have been identified as residing within a CrIS FOV (false negatives). The new code results in zero false negatives for most granules, although a few false negatives still occur in regions with highly variable terrain.

Another issue that the team addressed arose when a user found an artifact over warm, dry surfaces in the water vapor channels, i.e., fusion radiance channels constructed using the MODIS Band 27 & 28 response functions. The issue was that the channel 27 and 28 radiances showed signs of surface features, when none should be present for these channels. This was clearly an artifact of the VIIRS+CrIS fusion process. We found that we could mitigate the problem significantly, when water vapor band radiances are replaced with the split window (Band 31 and Band 32) brightness temperature differences in the *k-d* tree search. The split window BT differences are more sensitive to the layer above the surface than the surface itself. In Version 2.0, for the other channels than the water vapor ones, the same scaling as was applied for lat/lon has been applied for the radiances. As a result, the band specific MU factors have been eliminated. These changes mitigated the issue significantly but did not solve it entirely. The user should be aware that this issue may exist in dry slots where the water vapor loading is very low.

1.3 Quality flags and data use recommendations

Quality assurance (QA) flags in the level 2 products, sometimes also called confidence flags (CF), are used to identify if there is a possible problem with an individual retrieval. Examples of this include VIIRS granules in which the M15 and M16 radiance calibration was of bad quality, or when the CrIS data quality is poor.

The location and meanings of the QA flags within the files are described in Section 2.3.

1.4 Contact information and citation for data use

If you have general questions or comments regarding our data products, please email them to Dr. Eva Borbas, Dr. Elisabeth Weisz, or Dr. W. Paul Menzel (mailto:evab@ssec.wisc.edu; mailto:elisabeth.weisz@ssec.wisc.edu; mailto:paulm@ssec.wisc.edu). More information is also available on the VIIRS-CrIS Data Fusion project website (http://stc-se.com/data/bbaum/Baum-DataFusion), and the NASA data product site, https://ladsweb.modaps.eosdis.nasa.gov/missions-and-measurements/science-domain/viirs-cris-fusion/.

The VIIRS-CrIS IR absorption band data are available to the public without a monetary charge. If you use our data in a publication or report, we request that you read and cite the relevant paper(s) for the specific data set(s) used. The relevant data fusion papers include the following:

- Weisz, E., B. A. Baum, and W. P. Menzel, 2017: Fusion of satellite-based imager and sounder data to construct supplementary high spatial resolution narrowband IR radiances. *J. Appl. Remote Sens*. **11**(3), 036022 (2017), doi: 10.1117/1.JRS.11.036022.
- Cross, J. I. Gladkova, W. P. Menzel, A. Heidinger, and M. D. Grossberg, 2013: Statistical estimation of a 13.3-*μ*m Visible Infrared Imaging Radiometer Suite channel using multisensor data fusion. *J. Appl. Remote Sens*.**7**(1), 073473. doi: 10.1117/1.JRS.7.073473.
- Weisz, E. and W. P. Menzel, 2019: Imager and Sounder Data Fusion to Generate Sounder Retrieval Products at Improved Spatial and Temporal Resolution. *J. Appl. Remote Sens*. 13 (3), 034506.

Below are two recent papers that suggests that use of the fusion radiance product improves both cloud property retrievals and atmospheric water vapor products.

- Li, Y., Baum, B. A., Heidinger, A. K., Menzel, W. P., and Weisz, E., 2020: Improvement in cloud retrievals from VIIRS through the use of infrared absorption channels constructed from VIIRS-CrIS data fusion, *Atmos. Meas. Tech.*, **13**, 4035-4059, https://doi.org/10.5194/amt-13-4035-2020.

- Borbas, E. E., E. Weisz, C. Moeller, W. P. Menzel, and B. A. Baum: 2021: Improvement in tropospheric moisture retrievals from VIIRS through the use of infrared absorption bands constructed from VIIRS and CrIS data fusion. *Atmos. Meas. Tech.,* **14***,* 1191–1203*,* https://doi.org/10.5194/amt-14-1191-2021.

If a significant portion of our data is used in your publication, offers of co-authorship are also appreciated. In this case, please contact Dr. Eva Borbas (evab@ssec.wisc.edu).

In addition to citation, the following text can be used in an Acknowledgements or Data Availability section of a paper:

We thank the Data Fusion science team (http://stc-se.com/data/bbaum/Baum-DataFusion) for the VIIRS-CrIS IR absorption band data record.

2 Data organization

Level-2 (L2) files are available as 6-minute granules along the orbit track.

2.1 File naming convention

For L2 files, a sample filename is as follows for the NOAA-20 platform, broadly following the conventions familiar to users of MODIS data products:

FSNRAD_L2_VIIRS_CRIS_NOAA20.A2021208.1724.002.2021209215313.nc

The filename is interpreted as follows:

- **FSNRAD_L2_VIIRS_CRIS_NOAA20** indicates the ESDT of the product. The ESDT is separated into 4 components <product>_<level>_<sensors>_<satellite>. In this case this is the Fusion Radiances Level-2 product from a fusion of the VIIRS and CrIS sensors on the NOAA-20 (NOAA20) satellite.
- **A2021208** indicates the data acquisition year and day: YYYY represents the year followed by the day of year (DOY from 001 to 366) per the Julian calendar.
- **1724** indicates the time (HHMM UTC) at which the 6-minute long granule begins.
- **002** indicates the algorithm processing version, also known as 'Version' (here, Version 2.0).
- **2021209215313** indicates the date and time (UTC) at which the file was created (YYYY DOY per the Julian calendar HHMM).
- **nc** indicates a NetCDF4 file.

For fusion radiances constructed from VIIRS and CrIS on Suomi-NPP, the filename structure is the same but **NOAA20** is replaced with **SNPP**.

2.2 File format and structure

Each data file is in NetCDF format, compliant with climate and forecast (CF) conventions version 1.6. Each file contains multiple Scientific Data Sets (SDS), listed in Section 3.

2.3 L2 production, QC flags, and evaluation of radiances

Each L2 file contains data from a 6-minute portion of a single VIIRS+CrIS swath. We produce L2 fusion radiances at a resolution of the native VIIRS moderate-resolution (M) band pixels (i.e., 750m horizontal pixel size). The discussion of the QC flags that are provided for this product requires a basic understanding of the data fusion process. The following discussion provides a brief overview, with further details in Weisz et al. (2017).

To reduce confusion between the imager and sounder spatial resolution, we use "pixel" for the imager (750m for M-bands) and field-of-view, or "FOV" for the sounder (about 15 km). The construction of high spatial resolution IR narrowband radiances from VIIRS and CrIS data consists of two steps:

Step 1: Figure 3a shows the methodology involved with this part of the process. The basic point here is that a geolocation routine is used to match CrIS FOVs and VIIRS pixels. The geolocation step determines which VIIRS pixels are collocated with each large CrIS FOV. All of the VIIRS pixel high-spatial-resolution (HIRES) M15- and M16-band radiances collocated with a given CrIS FOV are averaged, so that there are low-spatial-resolution (LORES) M15 and M16 radiance values for each FOV.

Based on the high-resolution VIIRS M15 and M16 pixel radiances, and the averaged M15 and M16 radiances for each CrIS FOV, the k-d tree search finds the *N* sounder FOVs that best match each imager pixel. For the results shown here, *N* is set to 5. The k-d tree search algorithm is used to provide the closest matching FOVs in the training data set (here, low spatial resolution imager data) for each pixel in a query data set (here, high spatial resolution imager data). The corresponding imager and sounder latitude and longitude values are used as additional predictors. Specifically, the inputs to the k-d tree are the split- window 11 and 12 μm imager radiances at both the pixel and FOV spatial resolutions (HIRES and LORES, respectively), the number of pixels in an imager granule, and the geolocation for the radiances at the HIRES and LORES spatial resolutions (i.e., latitudes and longitudes). Note that the k-d tree search in this step is solely based on imager radiances (at the pixel resolution and averaged over the FOV resolution) and not on sounder radiances.

Step 2: For each of the *N* FOVs chosen as the best match for each VIIRS pixel in Step 1, we integrate over a set of specified spectral response functions to obtain a set of narrowband radiances. In this step, CrIS provides the spectral radiance measurements necessary to construct the fusion spectral bands for VIIRS. The mean of the convolved radiances for the *N* FOVs is computed; the mean radiance is what is provided to each VIIRS pixel as the fusion radiance. This process is repeated for every imager pixel in the granule.

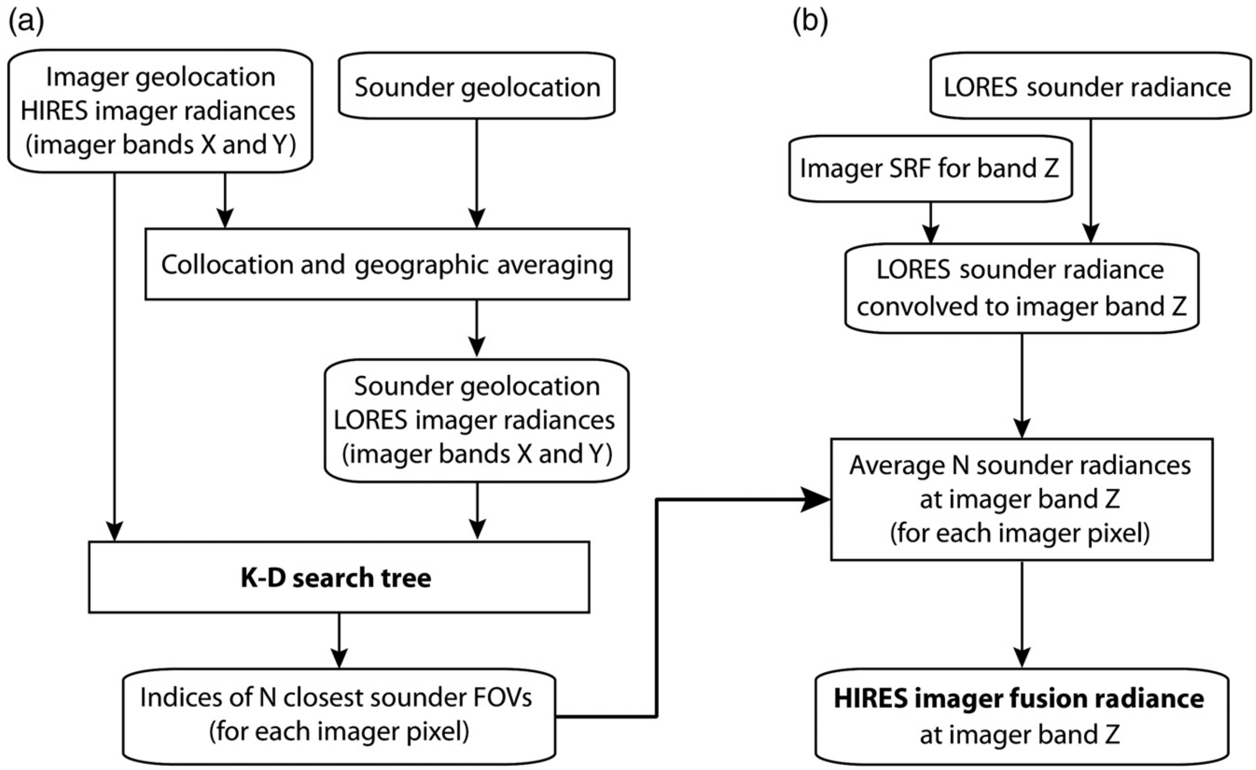

Figure 3: (a) The process for creating a multidimensional search tree using high spatial resolution (HIRES) and low spatial resolution (LORES) imager radiance and geolocation information. (b) Based on the k-d tree neighbor results, IR band radiances are constructed for each of the N CrIS FOVs selected as providing the closest radiance match for a given VIIRS pixel. The N radiances are averaged and stamped onto the VIIRS pixel. This process is repeated for each target IR radiance band for which a specified SRF (spectral response function) is given.

In each L2 data granule, the QC flags are intended to provide insight into the two steps in the data fusion process. The differences between Version 1.0.1 and 2.0 are noted here. In Version 1.0.1, the VIIRS granule quality check was performed for the entire granule. If more than 50% of the VIIRS pixels were not of sufficient quality, then the data fusion process was not run. The primary reason for this is that the geolocation process in Step 1 becomes suspect. In Version 2.0, this process was modified so that individual scanlines are checked for quality, rather than the entire granule. In the lunar calibration process (8-10 times per year), there are granules that are only partially affected, i.e., there may be a block of missing VIIRS scanlines, followed by a block of continuous scanlines for which calibration are available. We now process those granules that have continuous blocks of good data. When this occurs, the pixels that are missing data are filled with NaNs.

Black Body Warm-Up and Cool-Down (BB WUCD) operation is performed on a quarterly basis for S-NPP and occasionally for NOAA20 causing data gaps in the Fusion Radiance data coverage. According to SST group the impact on LW global brightness temperature mean is about 0.1K during this period, hence to increase the Fusion Radiance data coverage, processing during the BB WUCD operation (VIIRS Level-1B scan quality flag=32) is now added to fill the existing data gap.

If the data fusion process is run successfully, then other QC flags are provided based on the VIIRS and CrIS radiances. Three QC flags are provided for a subset of the VIIRS M bands listed in the global attribute called 'viirs_qc_bands'. Two VIIRS bands, M15 and M16, are used currently in the data fusion process in Step 1. For each of these VIIRS bands, a global attribute called viirs_qc_flag_meanings provides information on 'Missing_EV', 'Cal_Fail', and 'Fill', where Missing_EV means missing measurements from the Earth View (EV), Cal_Fail means calibration failure, and Fill means that pixels are given fill values. The values for these three QC flags are 65532, 65534, and 65535, respectively, in the global attribute called viirs_qc_flag_values.

To evaluate the percentage of pixels that are impacted by one of the three QC flags in 'viirs_qc_bands', there are 3 additional QC flags provided. The global attribute 'viirs_qc_missing_ev' provides a value for each of the bands in 'viirs_qc_bands', or M15 and M16, where 'ev' means Earth View. The value is given as a percentage of the pixels in the granule that have the value provided for 'Missing_EV'. In theory, the percentage ranges from 0 to 100.Similarly, the values provided in 'viirs_qc_cal_fail' and 'viirs_qc_fill' will range between 0 and 100. The user should be aware that if any of these three QC flags have high values, the fusion radiances could be suspect. To summarize, if the percentages provided for 'viirs_qc_missing_ev', 'viirs_qc_cal_fail' or 'viirs_qc_fill' are 0, this means that the VIIRS data for M15 and M16 are of the highest quality.

Based on the QC flags for the VIIRS bands used for data fusion (M15 and M16), and those provided in the CrIS Level-1B granules, the data fusion process is initiated. Subsequently, we provide the percentage of the pixels in the VIIRS granule where the fusion radiances are successfully created for each target fusion band. The target fusion bands are given in the global variable 'cris_qc_bands' and in the example are MODIS23, MODIS24, MODIS25, MODIS27, MODIS28, MODIS30, MODIS31, MODIS32, MODIS33, MODIS34, MODIS35, and MODIS36. The nomenclature used here means that the Aqua MODIS sensor's Spectral Response Functions (SRFs) were specified to generate fusion radiances. For example, MODIS33 means that the SRF for Aqua MODIS band 33 was used to convolve the CrIS radiances for the data fusion process.

In reference to Step 2, there are QC flags that pertain specifically to this part of the process. Basically, the question is: when the fusion radiances are generated, how good are the radiances based on the CrIS QC flags? The CrIS Level-1B granules provide 3 QC flags (variable: cris_qc_flag_meanings): Best, Good, and Do_Not_Use. The integer values for these flags is provided in cris_qc_flag_values as 0 (best), 1 (good), or 2 (worst), respectively. These QC flags are used to generate various absorption band radiances.

For each of the fusion bands listed in 'cris_qc_bands', currently numbering 12, a percentage (an integer) is provided in each of these 3 QC fields: cris_qc_best, cris_qc_good, and cris_qc_do_not_use. A value of '100', for example, for a band in cris_qc_best implies that 100%

of the pixels were successfully constructed based on the best CrIS data quality. However, if a value of ‘100’ is given for a band in cris_qc_do_not_use, this implies that 100% of the pixels were successfully constructed but were based on the worst CrIS data quality, and likely should not be used in your application.

An example of where the CrIS QC flags would be important is for the sensor on the Suomi-NPP platform for the period in 2019 when the mid-wave IR focal plane stopped working (about 2 months). The result of this focal plane issue is that MODIS27 and MODIS28 (6.7 and 7.3 μm, respectively) could not be constructed for VIIRS, but the other MODIS-like bands are still constructed and available for use.

2.4 Important note on fusion radiances that are constructed at high viewing angles

There is a long history of pairing an imager with a sounder on satellite polar-orbiting platforms, as shown in Figure 4. The salient point to note here is that the sounder sensor swath widths (HIRS, AIRS, CrIS, IASI) are always narrower than those of the imagers (AVHRR, MODIS, and VIIRS). In our VIIRS+CrIS fusion process, radiances are constructed for VIIRS outside of the CrIS swath, i.e., at scanning angles ≥ 60˚.

Sensor		Swath Width (km)
AVHRR	NOAA	2800
HIRS		2200
MODIS	Aqua	2330
AIRS		1650
VIIRS	S-NPP/NOAA-20	~3000
CrIS		2200
AVHRR	Metop-A/B/C	2800
HIRS/IASI		2200

Figure 4: Comparison of Imager (AVHRR, VIIRS, MODIS) and Sounder (HIRS, AIRS, CrIS, IASI) swath widths.

To gain insight as to the impact of not accounting for the increased atmospheric absorption outside of the CrIS swath, the fusion process was applied to MODIS and AIRS data for a granule, with results shown in Fig. 5.

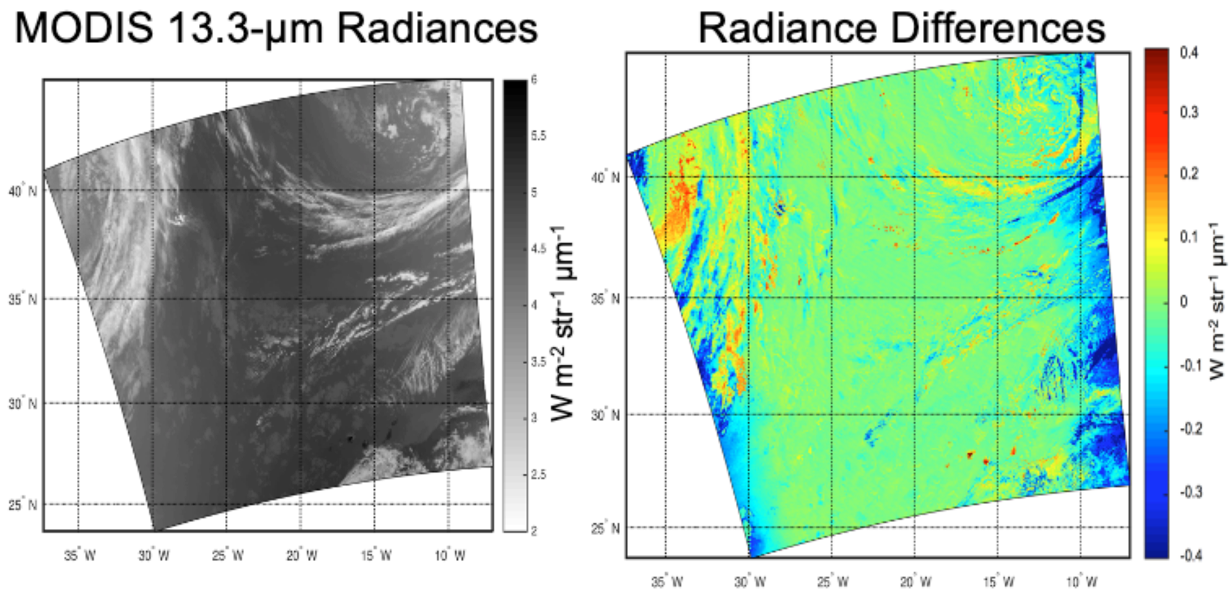

Figure 5: MODIS granule of 13.3-µm (Band 33) radiances from April 17, 2015 at 1435 UTC (left panel). The right panel shows the (MODIS-Fusion) 13.3-µm radiance differences. Note that the radiance differences increase modestly as the scan angle increases (where the radiance differences become negative), except for where there are clouds, which decrease the path length and hence the amount of water vapor absorption.

Outside of the CrIS swath, the fusion radiance product does not account for the additional absorption due to increased path length. After much discussion within the team, we decided that it was necessary to leave it up to the users to do this. There are multiple reasons that we considered, including that (a) the user needs to choose a product that provides the atmospheric moisture profile (e.g., from a sonde, numerical weather model or a sounder product from CrIS or AIRS), (b) choose a radiative transfer model for simulating the radiances that include consideration of the absorption, (c) decide what to do if there is a cloud in the pixel, which decreases the path length and hence absorption (Fig. 5 right panel), and (d) most importantly, if we chose to modify the radiances, it would be problematic for a user to remove the increased absorption from the fusion radiance product once the radiances are modified. The atmospheric profile can change depending on what you choose (ECMWF, MERRA-2, GDAS, etc), and radiative transfer models change over time. To know when there is a cloud in a pixel at the edge of the granules is also a concern, as cloud masking requirements/methodology are not uniform across the various scientific communities. For these reasons, each user must decide how best to account for the increased absorption outside of the CrIS swath.

3 Data content

Each L2 granule provides a number of constructed radiance spectral bands for both VIIRS and MODIS along with the information necessary to convert the radiances to brightness temperatures.

3.1 Dimensions

Three dimensions are defined within the L2 files:

- number_of_LUT_values, around 65536.
- number_of_lines, the index of the L2 cell in the along-track (roughly North-South) direction. This number is around 3248.
- number_of_pixels, the index of the L2 cell in the across-track (roughly East-West) direction. Denotes the number of pixels in a scan line, which is around 3200.

The radiances and brightness temperatures each have a defined size. The radiances are provided in a 2D array defined as (number of pixels, number of lines). The brightness temperature LUT is a 1D array defined as (number_of_LUT_values x 1).

3.2 Global attributes

The global attributes in the table below are present in the NOAA-20 L2 files. In a few cases, metadata are duplicated in multiple attributes to meet specific system needs or maintain data continuity with heritage sensors.

Attribute Name	Example
format_version	'1'
processing_level	'L2'
cdm_data_type	'swath'
creator email	‘sips.support@ssec.wisc.edu’
institution	'NASA Atmosphere SIPS'
project	‘NASA Atmosphere Discipline’
keywords_vocabulary	'NASA Global Change Master Directory (GCMD) Science Keywords'
license	'http://science.nasa.gov/earth-science/earth-science-data/data-information-policy/'
stdname_vocabulary	'NetCDF Climate and Forecast (CF) Metadata Convention'

naming_authority	'gov.nasa.gsfc.sci.atmos'
date_created	‘2021-07-28T21:35:50Z’
time_coverage_start	‘2021-07-27T17:24:00.000Z’
time_coverage_end	‘2021-07-27T17:30:00.000Z’
viirs_qc_flag_meanings	'Missing_EV, Cal_Fail, Fill'
viirs_qc_flag_values	65532US, 65534US, 65535US
viirs_qc_bands	'M15, M16'
viirs_qc_missing_ev	0US, 0US
viirs_qc_cal_fail	0US, 0US
viirs_qc_fill	0US, 0US
cris_qc_flag_meanings	'Best, Good, Do_Not_Use'
cris_qc_flag_values	0US, 1US, 2US
cris_qc_bands	'MODIS23, MODIS24, MODIS25, MODIS27, MODIS28, MODIS30, MODIS31, MODIS32, MODIS33, MODIS34, MODIS35, MODIS36'
cris_qc_best	100., 100., 100., 100., 100., 100., 100., 100., 100., 100., 100., 100.
cris_qc_good	0, 0, 0, 0, 0, 0, 0, 0, 0, 0, 0, 0
cris_qc_do_not_use	0, 0, 0, 0, 0, 0, 0, 0, 0, 0, 0, 0
conventions	'CF-1.6, ACDD-1.3'
platform	“NOAA-20’
creator_url	'https://sips.ssec.wisc.edu'
publisher_name	'LAADS'
publisher_email	'modis-ops@lists.nasa.gov'
publisher_url	'https://ladsweb.modaps.eosdis.nasa.gov/'
history	’Wed Jul 28 21:53:13 2021: ncks --fix_rec_dmn all -o FSNRAD_L2_VIIRS_CRIS_NOAA20.A2021208.1724.002.2021209215313.nc.tmp FSNRAD_L2_VIIRS_CRIS_NOAA20.A2021208.1724.002.2021209215313.nc\n’
product_name	‘FSNRAD_L2_VIIRS_CRIS_NOAA20.A2021208.1724.002.2021209215313.nc’
LocalGranuleID	‘FSNRAD_L2_VIIRS_CRIS_NOAA20.A2021208.1724.002.2021209215313.nc’
ShortName	‘FSNRAD_L2_VIIRS_CRIS_NOAA20’
product_version	‘2.0.0dev3’

AlgorithmType	‘OPS’
identifier_product_doi	‘10.5067/VIIRS/FSNRAD_L2_VIIRS_CRIS_NOAA20.002’
identifier_product_doi_aut	'http://dx.doi.org'
ancillary_files	' '
DataCenterId	'UWI-MAD/SSEC/ASIPS'
creator_institution	'Space Science & Engineering Center, University of Wisconsin - Madison'
publisher_institution	'NASA Level-1 and Atmosphere Archive & Distribution System'
GRingPointSequenceNo	1, 2, 3, 4
GRingPointLatitude	67.22364f, 83.19092f, 64.05853f, 55.94252f
GRingPointLongitude	-139.9146f, -12.15368f, -46.35101f, -100.4834f
geospatial_lat_units	'degrees_north'
geospatial_lon_units	'degrees_east'
geospatial_lat_min	55.94252f
geospatial_lat_max	85.44845f
geospatial_lon_min	-139.9146f
geospatial_lon_max	-12.15368f
NorthBoundingCoordinate	85.44845f
SouthBoundingCoordinate	55.94252f
EastBoundingCoordinate	-12.15368f
WestBoundingCoordinate	-139.9146f
startDirection	'Ascending'
endDirection	'Ascending'
OrbitNumber	19116
DayNightFlag	'Day'
NCO	‘netCDF Operators version 4.7.9 (Homepage = http://nco.sf.net, Code = http://github.com/nco/nco)’
_NCProperties	‘version=2,netcdf=4.6.2,hdf5=1.10.4’
instrument	'VIIRS+CrIS'
creator_name	'NASA Atmosphere SIPS'

title	‘NOAA20 VIIRS+CrIS Fusion (FSNRAD_L2_VIIRS_CRIS_NOAA20)’
long_name	‘NOAA20 VIIRS+CrIS Fusion 6-Min L2 Swath 750m'
processing_version	‘20210501-1’
viirs_l1_version	‘3.1.0dev’
viirs_lut_version	‘3.1.0.4’
viirs_lut_created	‘2021-04-14T00:00:00’
source	‘cris_l1 3.0.1, fusion_matlab 20210501-1, julia_cris_viirs 0.1.0, viirs_l1 3.1.0dev, viirsmend 1.2.12’
cris_l1_version	‘3.0.1’
input_files	‘VJ103MOD.A2021208.1724.021.2021209175010.uwssec.nc, VJ102MOD.A2021208.1724.021.2021209175659.uwssec.bowtie_restored.nc, SNDR.J1.CRIS.20210727T1724.m06.g175.L1B.std.v3_0_1.W.210727224915.nc’
xmlmetadata	‘<?xml version=\"1.0\"?>\n<!DOCTYPE GranuleMetaDataFile SYSTEM \"http://ecsinfo.gsfc.nasa.gov/ECSInfo/ecsmetadata/dtds/DPL/ECS/ScienceGranuleMetadata.dtd\">\n<GranuleMetaDataFile>\n <DTDVersion>1.0</DTDVersion>\n

3.3 Data field attributes

The attributes in the tables below are present for the SDS group called “geophysical_data” in the L2 files. One table is for the radiances and the M15 and M16 brightness temperature differences (BTD); the other is for the brightness temperature look-up table (LUT) associated with the radiances. The brightness temperature LUT is used to convert radiances to brightness temperatures.

The attributes for each radiance and BTD variable are in the following table:

Attribute name	**Description**	**Data type**
_FillValue	Value assigned to missing/invalid data	same type as data field
long_name	Long, descriptive name of data field	string
units	W m^{-2} μm^{-1} str^{-1} (“Watts/m^2/micrometer/steradian”)	string
valid_min	Minimum value to consider valid in the data	same type as data field

valid_max	Maximum value to consider valid in the data	same type as data field
scale_factor	Value assigned for the scale factor	float
add_offset	Value assigned for the offset	float
cris_qc_flag_meaning	"Best, Good, Do_Not_Use"	string
cris_qc_flag_percent	100., 0., 0.	float

The attributes for the brightness temperature LUT variable are as follows:

Attribute name	**Description**	**Data type**
_FillValue	Value assigned to missing/invalid data	same type as data field
units	“Kelvin”	string
long_name	Long, descriptive name of data field	string
valid_min	Minimum value to consider valid in the data	same type as data field
valid_max	Maximum value to consider valid in the data	same type as data field

3.4 SDS names and descriptions

3.4.1 Level-2 data fields

A number of variables are contained within these files. Each variable is for a specific wavelength band and has a related brightness temperature LUT. The following table groups related variables together.

For example, the brightness temperature can be calculated for MODIS Band 24 at pixel location (i,j) by:

$$BT24(i,j) = MODIS24\_brightness\_temperature\_lut(\ MODIS24\ (i,j)\ )$$

Note that there are SDSs for the brightness temperature differences (measured – constructed) for bands M15 and M16. These brightness temperature differences may be useful to methods that involve an optimal estimation approach, where some *a priori* estimate is required of uncertainties.

SDS name	Type	Description	Units
BTD_15	float	Difference of measured minus fusion VIIRS M15 brightness temperatures	Kelvin
BTD_16	float	Difference of measured minus fusion VIIRS M16 brightness temperatures	Kelvin
MODIS23	ushort	Radiances constructed for MODIS band 23 (2D)	$Wm^{-2}\mu m^{-1}str^{-1}$
MODIS23_brightness_temperature_lut	float	LUT to convert radiances to brightness temperatures for MODIS band 23 (2D)	Kelvin
MODIS24	ushort	Radiances constructed for MODIS band 24 (2D)	$Wm^{-2}\mu m^{-1}str^{-1}$
MODIS24_brightness_temperature_lut	float	LUT to convert radiances to brightness temperatures for MODIS band 24 (2D)	Kelvin
MODIS25	ushort	Radiances constructed for MODIS band 25 (2D)	$Wm^{-2}\mu m^{-1}str^{-1}$
MODIS25_brightness_temperature_lut	float	LUT to convert radiances to brightness temperatures for MODIS band 25 (2D)	Kelvin
MODIS27	ushort	Radiances constructed for MODIS band 27 (2D)	$Wm^{-2}\mu m^{-1}str^{-1}$
MODIS27_brightness_temperature_lut	float	LUT to convert radiances to brightness temperatures for MODIS band 27 (2D)	Kelvin
MODIS28	ushort	Radiances constructed for MODIS band 28 (2D)	$Wm^{-2}\mu m^{-1}str^{-1}$
MODIS28_brightness_temperature_lut	float	LUT to convert radiances to brightness temperatures for MODIS band 28 (2D)	Kelvin
MODIS30	ushort	Radiances constructed for MODIS band 30 (2D)	$Wm^{-2}\mu m^{-1}str^{-1}$
MODIS30_brightness_temperature_lut	float	LUT to convert radiances to brightness temperatures for MODIS band 30 (2D)	Kelvin
MODIS31	ushort	Radiances constructed for MODIS band 31 (2D)	$Wm^{-2}\mu m^{-1}str^{-1}$
MODIS31_brightness_temperature_lut	float	LUT to convert radiances to brightness temperatures for MODIS band 31 (2D)	Kelvin
MODIS32	ushort	Radiances constructed for MODIS band 32 (2D)	$Wm^{-2}\mu m^{-1}str^{-1}$
MODIS32_brightness_temperature_lut	float	LUT to convert radiances to brightness temperatures for MODIS band 32 (2D)	Kelvin
MODIS33	ushort	Radiances constructed for MODIS band 33 (2D)	$Wm^{-2}\mu m^{-1}str^{-1}$

MODIS33_brightness_temperature_lut	float	LUT to convert radiances to brightness temperatures for MODIS band 33 (2D)	Kelvin
MODIS34	ushort	Radiances constructed for MODIS band 34 (2D)	$Wm^{-2}\mu m^{-1}str^{-1}$
MODIS34_brightness_temperature_lut	float	LUT to convert radiances to brightness temperatures for MODIS band 34 (2D)	Kelvin
MODIS35	ushort	Radiances constructed for MODIS band 35 (2D)	$Wm^{-2}\mu m^{-1}str^{-1}$
MODIS35_brightness_temperature_lut	float	LUT to convert radiances to brightness temperatures for MODIS band 35 (2D)	Kelvin
MODIS36	ushort	Radiances constructed for MODIS band 36 (2D)	$Wm^{-2}\mu m^{-1}str^{-1}$
MODIS36_brightness_temperature_lut	float	LUT to convert radiances to brightness temperatures for MODIS band 36 (2D)	Kelvin

4 Reading the data

We use CF-compliant NetCDF4 to maximize the usability and accessibility of our data now and into the future. If you have trouble reading our data, or have suggestions on how to make it more useful, please contact us.

More information on NetCDF, including tools to access files in this format, is available at https://www.unidata.ucar.edu/software/netcdf/ . For quick browsing of the contents of individual files, the Panoply tool (http://www.giss.nasa.gov/tools/panoply/) provides a quick and easy interface. NetCDF libraries are also available in a variety of higher-level programming languages, such as IDL, Python, C/C++, and FORTRAN.

The Data Fusion website includes a page with more information about the content, assessment, and validation of the constructed IR absorption band radiances. More information is available at: http://stc-se.com/data/bbaum/Baum-DataFusion/index.html

5 Where to download the data

The data set is currently available through the NASA Level-1 and Atmosphere Archive & Distribution System (LAADS) at https://ladsweb.modaps.eosdis.nasa.gov/, which is the same place which hosts (among others) MODIS Deep Blue data products.

All data products are accessible from LAADS without a monetary charge, but users do need to register with NASA Earthdata and obtain a login account. First-time users who need to register may access the NASA User Registration System page via the following URL: https://urs.earthdata.nasa.gov

Users who may want to conduct a specific geographical/temporal search can do so via the LAADS Web search & order interface: https://ladsweb.modaps.eosdis.nasa.gov/search/

Remember to select the sensor (VIIRS/SNPP or VIIRS/NOAA20) and select the version before you define your spatial and temporal search parameters. If you have difficulties using the LAADS portal, please use the contact information on that webpage for support.

Acknowledgements

This research was funded by the ROSES Terra/Aqua/Suomi-NPP (TASNPP) program, managed by Hal Maring (NASA HQ). Data processing was performed at the Atmospheres Science Investigator-led Processing System (SIPS) at the University of Wisconsin, https://sips.ssec.wisc.edu. Data hosting resources were provided by the NASA LAADS at Goddard Space Flight Center

.

References

Scientific references about our data fusion algorithm development and validation are available on the website at http://stc-se.com/data/bbaum/Baum-DataFusion/index.html. Some key references that explain the algorithm and assessment of the radiances and resulting cloud products are additionally listed below:

- Weisz, E., B. A. Baum, and W. P. Menzel, 2017: Fusion of satellite-based imager and sounder data to construct supplementary high spatial resolution narrowband IR radiances. *J. Appl. Remote Sens*. 11(3), 036022 (2017), doi: 10.1117/1.JRS.11.036022.
- Cross, J. I. Gladkova, W. P. Menzel, A. Heidinger, and M. D. Grossberg, 2013: Statistical estimation of a 13.3-*μ*m Visible Infrared Imaging Radiometer Suite channel using multisensor data fusion. *J. Appl. Remote Sens*. **7** (1), 073473. doi: 10.1117/1.JRS.7.073473.